HHS Public Access

Author manuscript

Toxicol Appl Pharmacol. Author manuscript; available in PMC 2025 January 01.

Published in final edited form as:

Toxicol Appl Pharmacol. 2024 January ; 482: 116787. doi:10.1016/j.taap.2023.116787.

Arsenic up-regulates PD-L1 and enhances lung tumorigenesis through activation of STAT3 in alveolar epithelial type 2 cells

Wenhua Xu[1,2], **Jiajun Cui**[3], **Abdulrahman M. Busayli**[1], **Tong Zhang**[4], **Gang Chen**[1,#]

[1]Department Pharmacology & Nutritional Sciences, University of Kentucky College of Medicine, Lexington, KY 40536, USA

[2]Department of Neurology, the First Affiliated Hospital of University of Science and Technology of China, Hefei, Anhui 230001, China

[3]Department of Biochemistry, College of Medicine, Yichun University, Yichun, Jiangxi 336000, China

[4]Department of General Medicine, the First People's Hospital of Yunnan Province Kunming, Yunnan 650032, China

Abstract

Arsenic is a carcinogen and chronic exposure to arsenic increases the risk of many cancers, including lung cancer. However, the underlying mechanism is not clear. Using A/J mice as a model, our previous animal study has shown that chronic arsenic exposure up-regulates PD-L1 on lung tumor cells which interacts with PD-1 on T cells and inhibits T cell anti-tumor function resulting in increased lung tumorigenesis. In a subsequent *in vitro* study, we further found that arsenic up-regulated PD-L1 by activating STAT3 at tyrosine 705 in lung epithelial cells, and inhibition of STAT3 mitigated arsenic-induced PD-L1 up-regulation. The present study aims to determine whether STAT3 regulates PD-L1 in the lung of A/J mice and the type of cells from which lung tumor develops upon arsenic exposure. For that purpose, a mouse line with STAT3 conditional knockout in alveolar type 2 (AT2) cells was developed. Our results indicate that arsenic exposure up-regulates PD-L1 in AT2 cells through activating STAT3 in A/J mice. Conditional knockout of STAT3 in AT2 cells inhibited arsenic-induced PD-L1 up-regulation and lung tumor formation. Thus, our findings reveal that STAT3 is the upstream regulator of arsenic-induced PD-L1 up-regulation in AT2 cells and the inhibition of T cell anti-tumor function in the lung, and that AT2 cells are sensitive to arsenic exposure and from which arsenic-enhanced lung tumor formation in A/J mice.

Keywords

arsenic; mice; lung; tumor; tumorigenesis; STAT3; PD-L1

[#]To whom correspondence should be addressed at Department of Pharmacology & Nutritional Sciences, University of Kentucky College of Medicine, MN306, UKMC, 800 Rose St., Lexington, KY 40536. Fax: (859) 257-0077. gangchen6@uky.edu.

Introduction

Lung cancer stands as the second most prevalent cancer worldwide, afflicting both men and women. More than 230,000 lung cancer cases have been reported in the US in 2022. Among its subtypes, lung adenocarcinoma is the most frequent, accounting for approximately 40% of all lung cancer cases. The genesis of lung adenocarcinoma can be traced to the epithelial cells lining the alveoli. These cells fall into two categories: alveolar type 1 (AT1) and alveolar type 2 (AT2) cells. AT1 cells, with their flat and elongated morphology, possess limited regenerative capabilities, while AT2 cells exhibit a more cuboidal shape and a higher capacity for regeneration. These AT2 cells, typically expressing Surfactant Protein C (SP-C), have been thought to be involved in lung cancer initiation (Lin, Song et al. 2012, Xu, Rock et al. 2012, Sainz de Aja, Dost et al. 2021).

Arsenic, a recognized carcinogen, escalates the risk of various cancers, including lung cancer, following chronic exposure. The World Health Organization (WHO) has set a guideline value of 10 ppb as the maximum allowable concentration of arsenic in drinking water. However, certain regions, such as in Central, South, and Southeast Asia, parts of Africa, and North and South America, have naturally high levels of arsenic in groundwater, ranging from 100 to 300 ppb, with the highest recorded levels reaching up to 4700 ppb (Ahmad, Khan et al. 2018). Consequently, an estimated 140 million people worldwide have been drinking water containing arsenic at levels above the guideline value (Podgorski and Berg 2020). Meanwhile, the precise mechanism through which arsenic promotes lung cancer, as well as the specific cell type from which arsenic-induced lung cancer originates, remains elusive.

In previous study, utilizing a mouse model we demonstrated that chronic arsenic exposure can promote lung cancer, especially adenocarcinoma, by inhibiting T cell anti-tumor immunity via the activation of immune checkpoint pathways such as the PD-1/PD-L1 pathway (Xu, Cui et al. 2021). Arsenic exposure up-regulates the expression of Programmed Death-Ligand 1 (PD-L1) on tumor cells, which binds to its receptor, Programmed Death-1 (PD-1), on CD8 T cells, thus inhibiting the anti-tumor activity of these T cells in mouse lung. Our following *in vitro* investigation suggested that Signal Transducer and Activator of Transcription 3 (STAT3) may regulate arsenic-induced PD-L1 up-regulation on lung epithelial cells (Wang, Li et al. 2022). Nevertheless, whether STAT3 mediates this PD-L1 up-regulation, and in which type of cells arsenic augments PD-L1 expression *in vivo*, inducing cell transformation that leads to tumor formation, remain unclear.

The A/J inbred mouse strain, predisposed to adenocarcinoma following carcinogen exposure, displays a relatively high incidence of spontaneous adenoma/adenocarcinoma (Gunning, Castonguay et al. 1991, Kumar, Patlolla et al. 2016). Pathological analyses carried out by Cui and our team on these mice have revealed an augmented incidence and multiplicity of lung tumors, coupled with an inclination toward poorly differentiated lung adenocarcinoma (Cui, Wakai et al. 2006, Xu, Cui et al. 2021) upon long-term arsenic exposure. Therefore, A/J mice offer a valuable model for unraveling the mechanisms underlying arsenic-enhanced lung tumorigenesis.

Deciphering the type of cells that are sensitive to arsenic toxicity can yield pivotal insights into arsenic carcinogenicity. Given that the majority of lung tumors induced by arsenic in the A/J model are situated in the alveoli (Xu, Cui et al. 2021), which predominantly consist of alveolar epithelial cells, we generated a mouse line in the A/J background featuring a conditional knockout (KO) of STAT3 in AT2 cells. Our goal was twofold: 1) to determine the role of STAT3 in arsenic-induced PD-L1 up-regulation in the lung, and 2) to identify the alveolar epithelial cell subset from which arsenic may enhance tumor formation. Our findings indicate that arsenic exposure up-regulates PD-L1 expression in AT2 cells through STAT3 activation in the lung of A/J mice. Conditional STAT3 KO in AT2 cells inhibits arsenic-induced PD-L1 up-regulation and lung tumor formation. Importantly, our results indicate that STAT3 functions as the upstream regulator of arsenic-triggered PD-L1 up-regulation in AT2 cells and T cell anti-tumor dysfunction, and that AT2 cells are sensitive to arsenic exposure and from which arsenic-enhanced lung tumor formation in A/J mice.

Materials and Methods

1. Generation of a mouse line in which STAT3 is conditional knocked out in AT2 cells

All experimental procedures were approved by the Institutional Animal Care and Use Committee (IACUC) of the University of Kentucky. Mice were housed in individually ventilated cages and maintained a 12-hour light/12-hour dark cycle and standard conditions (21 ± 1.0°C and 50% humidity), with ad libitum access to food and water in the animal facility of the University of Kentucky. At the end of experiment, the mice were sacrificed under anesthesia with a mixture 200 mg/kg ketamine and 20 mg/kg xylazine.

The STAT3 floxed mice (B6.129S1-STAT3^{tm1Xyfu}/J, strain#: 016923) and AT2-Cre mice (B6.129S-*Sftpc*$^{tm1(cre/ERT2)Blh}$/J, strain#: 028054) were obtained from the Jackson Laboratories, both of which were in C57BL/6J background. To convert these mice to A/J background, AT2$^{Cre/Cre}$ male mice and STAT3$^{fl/fl}$ male mice were respectively mated with A/J female mice (A/J, Strain #:000646). The genotypes of offspring were determined by standard PCR protocols as suggested by the Jackson Laboratory. Briefly, the primers used for examining STAT3 floxed mice are: forward: 5'-TTG ACC TGT GCT CCT ACA AAA A-3'; reverse: 5'- CCC TAG ATT AGG CCA GCA CA-3'. The primers used for examining AT2-Cre mice are: mutant reverse: 5'-ACA CCG GCC TTA TTC CAA G-3'; common: 5'-TGC TTC ACA GGG TCG GTA G-3'; wild type reverse: 5'-CAT TAC CTG GGG TAG GAC CA-3'. The male heterozygous progeny were mated with A/J female mice, and this process was repeated over five generations to establish the A/J strain (Reilly 2016). Subsequently, the heterozygote siblings were paired, and homozygous offspring of STAT3$^{fl/fl}$ and AT2$^{Cre/Cre}$ were generated.

Male AT2$^{Cre/Cre}$ mice were crossed with female STAT3$^{fl/fl}$ mice, and two heterozygous offspring AT2$^{Cre/+}$ STAT3$^{fl/+}$ were intercrossed to yield mice that were hemizygous for the Cre transgene and homozygous for the STAT3 floxed allele (STAT3$^{fl/fl}$), leading to the development of AT2$^{Cre/+}$; STAT3$^{fl/fl}$ mice (Grisouard, Shimizu et al. 2015, Sandlesh, Juang et al. 2018). To create a mouse line with conditional KO of STAT3 in AT2 cells, 6 week-old AT2$^{Cre/+}$; STAT3$^{fl/fl}$ mice were intraperitoneally injected with tamoxifen solution (Sigma, 20

mg/mL in corn oil) at the dosage of 1 mg/day for a total of 5 consecutive days (Reinert, Kantz et al. 2012, Donocoff, Teteloshvili et al. 2020), which was repeated at age of 6-month old. The mice were monitored daily during tamoxifen treatment and their body weights were measured and compared before and after tamoxifen treatment. No considerable side effects and no mortality or substantial morbidity were observed in these tamoxifen-exposed mice.

2. Verification of conditional KO of STAT3 in AT2 cells

To examine if STAT3 has been knocked out in AT2 cells upon tamoxifen treatment, $AT2^{Cre/+}$: $STAT3^{fl/fl}$ mice were sacrificed 7 days after tamoxifen treatment, and lung tissue were harvested. Deletion of STAT3 in AT2 cells was verified by double labeling surfactant protein C (SP-C, the cell marker of AT2 cells) and STAT3 antibody to detect cell-specific STAT3 KO (Xu, Rock et al. 2012, Frank, Penkala et al. 2019). Briefly, Lung tissues fixed in 4% paraformaldehyde (PAF) were embedded in paraffin and cut into 5μm sections. Sections selected were deparaffinized with xylene and rehydrated through a graded series of ethanol, and then incubated in an antigen retrieval solution (Histo-VT One, Nacalai USA) for 30 min at 90°C. Rinsed three times in 0.1 M PBS, pre-incubated in the blocking solution containing 0.4% Triton-X-100 and 5% normal goat serum in 0.1 M PBS for 1 h at room temperature, and then the sections were incubated with the primary antibodies: rabbit anti–pro-SP-C (1:500, AB3786, Millipore), and mouse anti-STAT3 (1:500, #9139, Cell Signaling) at 4°C overnight. The following day, the sections were rinsed five times in 0.1 M PBS and incubated with secondary antibodies: Alexa Fluor™594 goat anti-rabbit IgG (1:500, A21207, Invitrogen), and Alexa Fluor™488 goat anti-mouse IgG (1:500, A11001, Invitrogen) for 1 hr at room temperature in a dark place. After rinsing five times in 0.1 M PBS, the sections were mounted with ProLong™ Gold Antifade Mountant with DAPI (P36931, Thermo Fisher Scientific) and then ready for immunofluorescent imagine analysis.

3. Animal arsenic treatment

In this study, a previously published mouse model was used, in which A/J mice were treated with 500 ppb arsenic in drinking water and lung tumorigenesis was enhanced (Xu, Cui et al. 2021). Briefly, wild type and STAT3 conditional KO in AT2 cells A/J mice at the age of 8 weeks, even in sex, were randomly assigned to four treatment groups (20 mice/group): distilled water feeding wild-type A/J mice control group (Ct), distilled water feeding STAT3 conditional KO mice group ($STAT3^{KO}$), arsenic treatment (500 ppb of sodium arsenite, Sigma) wild-type A/J mice group (As), and arsenic treatment STAT3 conditional KO mice group ($STAT3^{KO}$-As) for 12 months. Cre-negative littermates of conditional KO mice treated with tamoxifen, same as the KO mice, were used as tamoxifen treatment control (T-Ct). Food and water (with or without arsenic) were available ad libitum throughout the study and the mice showed no apparent differences among the groups (Xu, Cui et al. 2021).

4. Histology, immunohistochemistry and immunofluorescence procedures

For histological analysis, lung tissues from different treatment groups were collected, fixed with 4% PFA, embedded in paraffin, cut into sections (5μm), and then stained with hematoxylin and eosin (H&E, Scy Tek, HMM500 & EYQ500). For immunohistochemistry or fluorescence colocalization staining, lung tissue sections from different groups were subjected to antigen retrieval using 1X Histo-VT One (#06380-05, Nacalai USA) for 30

min at 90 °C as previously described (Xu, Cui et al. 2021). After rinsing 3 times in 0.1 M PBS each for 10 min, the sections were pre-incubated with a blocking buffer containing 5% normal goat serum and 0.4% Triton-X-100 in 0.1 M PBS for 1 hour at room temperature. To investigate the epithelial type of tumor cells, some sections were respectively incubated with the primary antibodies: rabbit uteroglobin/CC10 polyclonal antibody (1:500, 10490-1-AP, Proteintech), rabbit anti–pro-SP-C (1:500, AB3786, Millipore), rabbit aquaporin-5 (AQP5) antibody (1:200, #20105, BiCell). After rinsing 4 times in 0.1 M PBS, the sections were incubated with biotinylated anti-rabbit IgG (1:500, BA-1000, Vector Laboratories) for 1 hour at room temperature. The sections were rinsed 5 times in 0.1 M PBS and treated for 30 min with a solution of avidin-biotin complex (PK-4000, Vectastain ABC Elite kit, Vector Laboratories). The sections were then rinsed 3 times in 0.1 M PB and incubated with the working solution of Vector® DAB Peroxidase Substrate (#SK-4100, Vector Laboratories) for 5 min. After staining, the sections were dehydrated in graded ethanol, clear in xylene, and mounted with a coverslip. Fluorescence colocalization was used for qualitative and quantitative analysis. Lung tissue sections were first subjected to antigen retrieval and blocking non-specific binding, and then incubated with the first primary antibody. To verify the conditional KO of STAT3 in AT2 cells, some sections were incubated with rabbit anti–pro-SP-C (1:500, AB3786, Millipore) and mouse anti-STAT3 (1:500, #9139, Cell Signaling) at 4°C overnight. To examine the expression of p-Stat3 in the AT2 cells, some sections were incubated with rabbit anti-pro-SP-C (1:500, AB3786, Millipore) and mouse anti-phospho-STAT3 mAb (1:500, #9138, Cell Signaling) at 4°C overnight. Upon the completion of incubation with the primary antibodies, the sections were rinsed in 0.1 M PBS 5 times for 10 min each time. Then the sections for pro-SP-C and Stat3 colocalization were incubated with Alexa fluor-conjugated 594 donkey anti-rabbit IgG (1:500, A21207, Thermo Fisher Scientific) and Alexa fluor-conjugated 488 goat anti-mouse IgG (1:500, A11001, Thermo Fisher Scientific) for 1 hour at room temperature in dark place. The sections for pro-SP-C and p-STAT3 double staining were incubated with Alexa fluor-conjugated 488 donkey anti-rabbit IgG (1:500, A21206, Thermo Fisher Scientific) and Alexa fluor-conjugated 594 goat anti-mouse IgG (1:500, A11005, Thermo Fisher Scientific). After washing with 0.1 M PBS 10 times for 10 min each time, the sections were cover-slipped by ProLong™ Gold Antifade Mountant with DAPI (P36931, Thermo Fisher Scientific), and scanned under the Olympus BX61S Virtual Slide Microscope with Olympus VS120 Automated Slide Scanner software. Three fluorescent dyes were used to label these specific cell populations and quantify them with the help of fluorescence microscopy. 3 – 5 random fields for around 100 cells in each sample were analyzed. Since we found no sex differences in PD-L1 expression or tumorigenesis in both control and arsenic-treated groups of our previous study (Xu, Cui et al. 2021), mice even in sex were included for data analysis of the histology, immunohistochemistry and immunofluorescence experiments of current study.

5. Preparation of single cell suspensions for flow cytometry

For lung tissue dissociation, the digestion solution was freshly prepared as follows: 1.5 mg/ml of collagenase A (Sigma), 10 μg/ml of DNase I (Roche), and 10% FBS in Dulbecco's phosphate Buffered Saline (DPBS) with $MgCl_2$ and $CaCl_2$ (Sigma). The lung tissues were collected and processed rapidly after the mice were euthanized, minced with scissors into pieces no larger than 1 mm, and then placed in 5mL digestion solution and incubated at

37°C for 30 min with shaking at 250 rpm. After incubation, the dissociated lung tissues were filtered using a 100 μM cell strainer to remove the tissue debris, and the supernatants were carefully removed after centrifuged, ensuring not to disrupt the cell pellets. The cell pellets were re-suspended with 5 mL 1× RBC lysis buffer with 5 min incubation on ice, and then washed twice with 25 mL cold PBS with 1% BSA. The single cell suspensions were harvested by centrifugation, counted using an automated cell counter Countess™ (C10283, Invitrogen, Thermo Fisher Scientific), diluted in cold PBS containing 2% FCS at the concentration of 1×10^7 cell/mL for further analysis.

6. Flow cytometry analysis

Several cell surface markers such as PD-L1, CD45 (both from BioLegend) were used to identify and quantify different cell populations. CD45 was used to distinguish lung tissue cells ($CD45^-$) from infiltrating immune cells ($CD45^+$), followed by examination of $PD\text{-}L1^+$ and $PD\text{-}L1^-$ cells. For blocking non-specific binding of Fc receptors, the single cells were pre-incubated with purified anti-mouse CD16/CD32 antibody (BioLegend) for 15 min on ice prior to cell surface staining. The isotope controls matching the primary antibodies were used as negative controls. For Flow cytometric detection, 2 μL Zombie Yellow™ Fixable Viability solution (#423103, BioLegend) was added to each sample to exclude dead cells, and the viable cells were gated on a forward versus side scatter (FSC vs. SSC) plot to identify the cells of interest. Data were acquired using a BD Canto II cytometer equipped with Diva software and analyzed using FlowJo 11.0 version.

7. Statistical analysis

IBM SPSS 26 and GraphPad Prism 8 were used to analyze the data and create the bar graphs. Tumor incidence among different groups was compared with Crosstabs (Gliner, Morgan et al. 2002), and tumor multiplicity was analyzed by Poisson Regression (Blizzard and Hosmer 2006). Numerical data were presented as (mean ± SD) and analyzed by a factorial ANOVA. The effect size partial eta squared (η^2p) was calculated and reported, and post-hoc tests were run to explore differences between groups (McHugh 2011). Independent samples *t*-test was used to identify the significant difference between the control and arsenic-treated groups (Codonhato, Rubio et al. 2018). A p value ≤ 0.05 was considered statistically significant.

Results

1. Arsenic-promoted lung tumor cells exhibited the cell marker of AT2 cells in A/J mice

Since our previous study showed that arsenic promotes lung tumorigenesis in A/J mice (Xu, Cui et al. 2021), in current study we first sought to determine the cellular traits of arsenic-promoted lung tumor by immunohistochemistry. As shown in Fig. 1, the majority of the tumor cells expressed SP-C protein (the marker of AT2 cells), while much less of tumor cells expressed Aquaporin 5 (AQP5, the marker of AT1 cells), and none of them expressed CC10 (the marker of Clara cells). No differences were observed between male and female mice, or between the control and arsenic-treated groups (supplementary Figure 1). These observations suggest that arsenic-promoted lung tumor cells possess similar cellular characteristics of the AT2 cells as in control mice.

2. Arsenic exposure activated STAT3 in the AT2 cells

Given that our previous *in vitro* study has found that arsenic up-regulated PD-L1 by activating STAT3 at tyrosine 705 in BEAS-2B cells (Wang, Li et al. 2022), our subsequent step examined if arsenic activated STAT3 within AT2 cells of A/J mice by immunofluorescent image analysis. As shown in Fig. 2, arsenic exposure increased the co-localization of phosphorylated STAT3 with SP-C staining in the alveoli compared to the control group. This data suggests that arsenic may activate STAT3 in AT2 cells.

3. STAT3 mediates arsenic-induced PD-L1 upregulation in AT2 cells

Our previous animal study showed that arsenic promoted lung tumorigenesis through upregulating PD-L1 resulting in activation of PD-L1/PD-1 immune checkpoint pathway and inhibition of T cell anti-tumor immunity (Xu, Cui et al. 2021). To explore if arsenic up-regulates PD-L1 through activating STAT3 in AT2 cells of A/J mice, we used the Cre/loxP system to generate an A/J mouse line in which STAT3 was conditionally knocked out in AT2 cells upon tamoxifen treatment. The AT2-Cre (B6.129S-*Sftpc*$^{tm1(cre/ERT2)Blh}$/J) mice and STAT3$^{fl/fl}$ (B6.129S1-STAT3^{tm1Xyfu}/J) mice were first converted to A/J background by crossing, respectively, with wild type A/J mice for 5 generations. Then, their offspring were intercrossed to obtain AT2$^{Cre/+}$; STAT3$^{fl/fl}$ mice. Immunofluorescence assay data demonstrated that the number of STAT3^{+} AT2 cells was significantly reduced in the mice treated with tamoxifen compared to the wild type A/J mice, which verifies that the STAT3 was knocked out in AT2 cells of these mice (Fig. 3A). Since our previous study indicated that arsenic upregulated PD-L1 on lung tissue cells contributed to arsenic-enhanced lung tumorigenesis in A/J mice (Xu, Cui et al. 2021). We subsequently used the STAT3 conditional KO mice to examine the PD-L1 levels in the lung tissue cells with or without arsenic exposure by flow cytometry and compared to those in wildtype mice. As shown in Fig. 3B, arsenic-induced PD-L1 up-regulation on lung tissue cells was significantly inhibited in STAT3 conditional KO mice, further indicating that arsenic up-regulates PD-L1 on AT2 cells through activating STAT3.

4. Arsenic-enhanced lung tumorigenesis was mitigated in the A/J mice with STAT3 KO in AT2 cells

Finally, we determined if activation of STAT3/PD-L1 in AT2 cells contribute to arsenic-enhanced lung tumorigenesis in A/J mice. Wild type mice and the STAT3 conditional KO mice were fed with drinking water with or without arsenic and lung tumor formation was examined 12-month later as performed in our previous study (Xu, Cui et al. 2021). Cre-negative littermates of conditional KO mice treated with tamoxifen, same as the KO mice, were also included as treatment control. As shown in Table 1, arsenic-increased both lung tumor incidence rate and multiplicity were significantly mitigated by STAT3 KO in AT2 cells. The results presented here and above indicate that activation of STAT3/PD-L1 in AT2 cells contributes to arsenic-induced lung tumor formation.

Discussion

A/J mice have been widely used for lung tumor study, while C57BL/6 is resistant to lung tumorigenesis (Dassano, Colombo et al. 2014). In the current study, an A/J mouse line

with conditional KO of STAT3 in AT2 cells was generated by using the Cre/loxP system. Using this mouse model, our results showed that chronic arsenic exposure activated STAT3 and up-regulated PD-L1 in AT2 cells. Importantly, arsenic-induced up-regulation of PD-L1 was significantly mitigated in STAT3 conditional KO mice, suggesting that STAT3 is the upstream regulator of PD-L1 upon arsenic exposure. This result is in line with our prior *in vitro* study (Wang, Li et al. 2022), indicating that STAT3 plays a role in the up-regulation of PD-L1 in response to arsenic exposure.

We also investigated the impact of STAT3 deletion in AT2 cells on arsenic-enhanced lung tumorigenesis. While chronic arsenic exposure increased lung tumor incidence and multiplicity in wild type mice (Xu, Cui et al. 2021), conditional KO of STAT3 in AT2 cells inhibited arsenic-increased lung tumor burden (Table 1). This finding together with those from our previous studies reveal that arsenic-enhanced lung tumorigenesis in A/J mice was mediated by STAT3/PD-L1 in AT2 cells.

Aberrant activation of STAT3 has been associated with tumor progression and worse prognosis of patients with lung cancer (Harada, Takigawa et al. 2014, Tong, Wang et al. 2017). STAT3 is a transcription factor that regulates the expression of numerous genes involved in cell proliferation, survival, and immune response. Phosphorylation of STAT3 at tyrosine 705 and serine 727 is a crucial step in STAT3 activation that enables its dimerization, nuclear translocation, and DNA binding. While the phosphorylation of serine 727 maximizes the transcriptional activity of STAT3, the phosphorylation of tyrosine 705 is a key event in its activation and subsequent signaling in both normal and tumor cells (Tolomeo and Cascio 2021). Activated STAT3 binds to the promoter region of PD-L1 gene and initiates PD-L1 transcription in some tumors including lung tumor (Marzec, Zhang et al. 2008, Fujita, Yagishita et al. 2015, Song, Nairismagi et al. 2018, Zerdes, Wallerius et al. 2019, Lee, Lee et al. 2021, Chen, Zhuang et al. 2022). Up-regulated PD-L1 then interacts with PD-1 on CD8 T cells leading to immunosuppressive microenvironments and facilitating tumor growth (Bu, Yu et al. 2017). Previous study also showed that long term arsenic exposure induces STAT3 phosphorylation at tyrosine 705 which contributes significantly to arsenic-induced cell malignant transformation (Almutairy, Fu et al. 2022). The current study aligns well with those studies and further indicates that arsenic exposure increased the phosphorylated STAT3 at tyrosine 705 and up-regulated PD-L1 in AT2 cells of the lung and STAT3 KO in AT2 cells blocked arsenic-induced PD-L1 up-regulation and lung tumor formation. These findings highlight the importance of tyrosine 705 phosphorylation in arsenic-induced STAT3 activation and consequently PD-L1 up-regulation and lung tumor formation.

The results of current study also demonstrated that the AT2 cells may be sensitive to arsenic exposure and serve as the cellular origin of arsenic-promoted lung cancer, which has not been known before. AT2 cells are well-known for their stem cell-like properties: they can self-renew, differentiate into AT1 cells, and regenerate and repair lung tissues (Jacob, Vedaie et al. 2019). Our findings deepen the understanding of the cellular origin and the underlying mechanism of arsenic-promoted lung cancer. We may further determine the up-stream regulators of arsenic-induced STAT3 activation in the AT2 cells and examine the

efficacy of the specific inhibitors of STAT3 in prevention/treatment of arsenic-enhanced lung tumorigenesis in the future studies.

Supplementary Material

Refer to Web version on PubMed Central for supplementary material.

Acknowledgment:

We would like to thank Dr. Wendy Katz for histology service and Dr. Kate Kosmac for assistance with Microscopy.

Funding:

This work was supported by NIH grants ES026657 to GC and P30CA177558 to the Shared Resource Facilities of the University of Kentucky Markey Cancer Center.

Declaration of interests

Gang Chen reports financial support was provided by National Institutes of Health.

References

Ahmad SA, Khan MH and Haque M (2018). "Arsenic contamination in groundwater in Bangladesh: implications and challenges for healthcare policy." Risk Manag Healthc Policy 11: 251–261. [PubMed: 30584381]

Almutairy B, Fu Y, Bi Z, Zhang W, Wadgaonkar P, Qiu Y, Thakur C and Chen F (2022). "Arsenic activates STAT3 signaling during the transformation of the human bronchial epithelial cells." Toxicol Appl Pharmacol 436: 115884. [PubMed: 35031324]

Blizzard L and Hosmer DW (2006). "Parameter estimation and goodness-of-fit in log binomial regression." Biom J 48(1): 5–22. [PubMed: 16544809]

Bu LL, Yu GT, Wu L, Mao L, Deng WW, Liu JF, Kulkarni AB, Zhang WF, Zhang L and Sun ZJ (2017). "STAT3 Induces Immunosuppression by Upregulating PD-1/PD-L1 in HNSCC." J Dent Res 96(9): 1027–1034. [PubMed: 28605599]

Chen Q, Zhuang S, Hong Y, Yang L, Guo P, Mo P, Peng K, Li W, Xiao N and Yu C (2022). "Demethylase JMJD2D induces PD-L1 expression to promote colorectal cancer immune escape by enhancing IFNGR1-STAT3-IRF1 signaling." Oncogene 41(10): 1421–1433. [PubMed: 35027670]

Codonhato R, Rubio V, Oliveira PMP, Resende CF, Rosa BAM, Pujals C and Fiorese L (2018). "Resilience, stress and injuries in the context of the Brazilian elite rhythmic gymnastics." PLoS One 13(12): e0210174. [PubMed: 30596793]

Cui X, Wakai T, Shirai Y, Hatakeyama K and Hirano S (2006). "Chronic oral exposure to inorganic arsenate interferes with methylation status of p16INK4a and RASSF1A and induces lung cancer in A/J mice." Toxicol Sci 91(2): 372–381. [PubMed: 16543296]

Dassano A, Colombo F, Trincucci G, Frullanti E, Galvan A, Pettinicchio A, De Cecco L, Borrego A, Martinez Ibanez OC, Dragani TA and Manenti G (2014). "Mouse pulmonary adenoma susceptibility 1 locus is an expression QTL modulating Kras-4A." PLoS Genet 10(4): e1004307. [PubMed: 24743582]

Donocoff RS, Teteloshvili N, Chung H, Shoulson R and Creusot RJ (2020). "Optimization of tamoxifen-induced Cre activity and its effect on immune cell populations." Sci Rep 10(1): 15244. [PubMed: 32943672]

Frank DB, Penkala IJ, Zepp JA, Sivakumar A, Linares-Saldana R, Zacharias WJ, Stolz KG, Pankin J, Lu M, Wang Q, Babu A, Li L, Zhou S, Morley MP, Jain R and Morrisey EE (2019). "Early lineage specification defines alveolar epithelial ontogeny in the murine lung." Proc Natl Acad Sci U S A 116(10): 4362–4371. [PubMed: 30782824]

Fujita Y, Yagishita S, Hagiwara K, Yoshioka Y, Kosaka N, Takeshita F, Fujiwara T, Tsuta K, Nokihara H, Tamura T, Asamura H, Kawaishi M, Kuwano K and Ochiya T (2015). "The clinical relevance

of the miR-197/CKS1B/STAT3-mediated PD-L1 network in chemoresistant non-small-cell lung cancer." Mol Ther 23(4): 717–727. [PubMed: 25597412]

Gliner JA, Morgan GA and Harmon RJ (2002). "The chi-square test and accompanying effect size indices." J Am Acad Child Adolesc Psychiatry 41(12): 1510–1512. [PubMed: 12447039]

Grisouard J, Shimizu T, Duek A, Kubovcakova L, Hao-Shen H, Dirnhofer S and Skoda RC (2015). "Deletion of Stat3 in hematopoietic cells enhances thrombocytosis and shortens survival in a JAK2V617F mouse model of MPN." Blood 125(13): 2131–2140. [PubMed: 25595737]

Gunning WT, Castonguay A, Goldblatt PJ and Stoner GD (1991). "Strain A/J mouse lung adenoma growth patterns vary when induced by different carcinogens." Toxicol Pathol 19(2): 168–175. [PubMed: 1771369]

Harada D, Takigawa N and Kiura K (2014). "The Role of STAT3 in Non-Small Cell Lung Cancer." Cancers (Basel) 6(2): 708–722. [PubMed: 24675568]

Jacob A, Vedaie M, Roberts DA, Thomas DC, Villacorta-Martin C, Alysandratos KD, Hawkins F and Kotton DN (2019). "Derivation of self-renewing lung alveolar epithelial type II cells from human pluripotent stem cells." Nat Protoc 14(12): 3303–3332. [PubMed: 31732721]

Kumar G, Patlolla JM, Madka V, Mohammed A, Li Q, Zhang Y, Biddick L, Singh A, Gillaspy A, Lightfoot S, Steele VE, Kopelovich L and Rao CV (2016). "Simultaneous targeting of 5-LOX-COX and ODC block NNK-induced lung adenoma progression to adenocarcinoma in A/J mice." Am J Cancer Res 6(5): 894–909. [PubMed: 27293987]

Lee JH, Lee DY, Lee HJ, Im E, Sim DY, Park JE, Park WY, Shim BS and Kim SH (2021). "Inhibition of STAT3/PD-L1 and Activation of miR193a-5p Are Critically Involved in Apoptotic Effect of Compound K in Prostate Cancer Cells." Cells 10(8).

Lin C, Song H, Huang C, Yao E, Gacayan R, Xu SM and Chuang PT (2012). "Alveolar type II cells possess the capability of initiating lung tumor development." PLoS One 7(12): e53817. [PubMed: 23285300]

Marzec M, Zhang Q, Goradia A, Raghunath PN, Liu X, Paessler M, Wang HY, Wysocka M, Cheng M, Ruggeri BA and Wasik MA (2008). "Oncogenic kinase NPM/ALK induces through STAT3 expression of immunosuppressive protein CD274 (PD-L1, B7-H1)." Proc Natl Acad Sci U S A 105(52): 20852–20857. [PubMed: 19088198]

McHugh ML (2011). "Multiple comparison analysis testing in ANOVA." Biochem Med (Zagreb) 21(3): 203–209. [PubMed: 22420233]

Podgorski J and Berg M (2020). "Global threat of arsenic in groundwater." Science 368(6493): 845–850. [PubMed: 32439786]

Reilly KM (2016). "Controlling Genetic Background in Crosses of Mouse Models of Cancer." Cold Spring Harb Protoc 2016(3): pdb prot079160.

Reinert RB, Kantz J, Misfeldt AA, Poffenberger G, Gannon M, Brissova M and Powers AC (2012). "Tamoxifen-Induced Cre-loxP Recombination Is Prolonged in Pancreatic Islets of Adult Mice." PLoS One 7(3): e33529. [PubMed: 22470452]

Sainz de Aja J, Dost AFM and Kim CF (2021). "Alveolar progenitor cells and the origin of lung cancer." J Intern Med 289(5): 629–635. [PubMed: 33340175]

Sandlesh P, Juang T, Safina A, Higgins MJ and Gurova KV (2018). "Uncovering the fine print of the CreERT2-LoxP system while generating a conditional knockout mouse model of Ssrp1 gene." PLoS One 13(6): e0199785. [PubMed: 29953487]

Song TL, Nairismagi ML, Laurensia Y, Lim JQ, Tan J, Li ZM, Pang WL, Kizhakeyil A, Wijaya GC, Huang DC, Nagarajan S, Chia BK, Cheah D, Liu YH, Zhang F, Rao HL, Tang T, Wong EK, Bei JX, Iqbal J, Grigoropoulos NF, Ng SB, Chng WJ, Teh BT, Tan SY, Verma NK, Fan H, Lim ST and Ong CK (2018). "Oncogenic activation of the STAT3 pathway drives PD-L1 expression in natural killer/T-cell lymphoma." Blood 132(11): 1146–1158. [PubMed: 30054295]

Tolomeo M and Cascio A (2021). "The Multifaced Role of STAT3 in Cancer and Its Implication for Anticancer Therapy." Int J Mol Sci 22(2).

Tong M, Wang J, Jiang N, Pan H and Li D (2017). "Correlation between p-STAT3 overexpression and prognosis in lung cancer: A systematic review and meta-analysis." PLoS One 12(8): e0182282. [PubMed: 28797050]

Wang H, Li J, Xu W, Li C, Wu K, Chen G and Cui J (2022). “The mechanism underlying arsenic-induced PD-L1 upregulation in transformed BEAS-2B cells.” Toxicol Appl Pharmacol 435: 115845. [PubMed: 34953898]

Xu W, Cui J, Wu L, He C and Chen G (2021). “The role of PD-1/PD-L1 checkpoint in arsenic lung tumorigenesis.” Toxicol Appl Pharmacol 426: 115633. [PubMed: 34166680]

Xu X, Rock JR, Lu Y, Futtner C, Schwab B, Guinney J, Hogan BL and Onaitis MW (2012). “Evidence for type II cells as cells of origin of K-Ras-induced distal lung adenocarcinoma.” Proc Natl Acad Sci U S A 109(13): 4910–4915. [PubMed: 22411819]

Zerdes I, Wallerius M, Sifakis EG, Wallmann T, Betts S, Bartish M, Tsesmetzis N, Tobin NP, Coucoravas C, Bergh J, Rassidakis GZ, Rolny C and Foukakis T (2019). “STAT3 Activity Promotes Programmed-Death Ligand 1 Expression and Suppresses Immune Responses in Breast Cancer.” Cancers (Basel) 11(10).

Highlights

- Arsenic up-regulates PD-L1 through activating STAT3 in A/J mice.
- Arsenic increases the phosphorylation of STAT3 at tyrosine 705 in lung AT2 cells.
- Arsenic-promoted lung tumor cells exhibit the cell marker of AT2 cells.
- STAT3 mediates arsenic-induced PD-L1 up-regulation in AT2 cells and lung tumorigenicity.

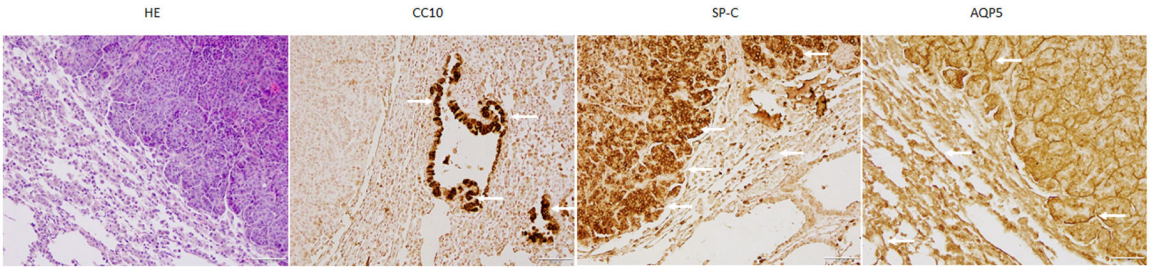

Figure 1. Arsenic-promoted lung tumor cells exhibited characteristics resembling AT2 cells in A/J mice.

Lung tissue samples were stained with SP-C (the marker protein of AT2 cells), AQP5 (the marker for AT1 cells) and CC10 (the marker of Clara cells). The majority of the tumor cells are cuboidal AT2 cells expressed SP-C, while much less are thin, flat AT1 cells expressed AQP5. Since no noticeable differences were observed between treatment groups or between sexes, only pictures from male mice in arsenic-treated group are shown. Arrows indicate the positive staining of the relative antibodies.

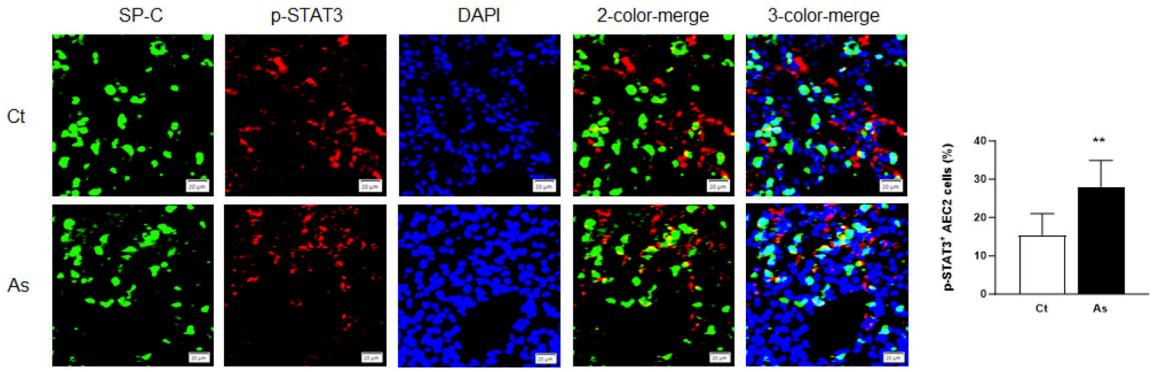

Figure 2. Arsenic exposure activated STAT3 in the AT2 cells.

Lung tissue samples were stained with antibodies against SP-C and phosphorylated STAT3 at tyrosine 705. Arsenic treatment (As) significantly increased the number of cells with the merged staining of these two antibodies compared to control (Ct) group. N=8. **: $p < 0.01$.

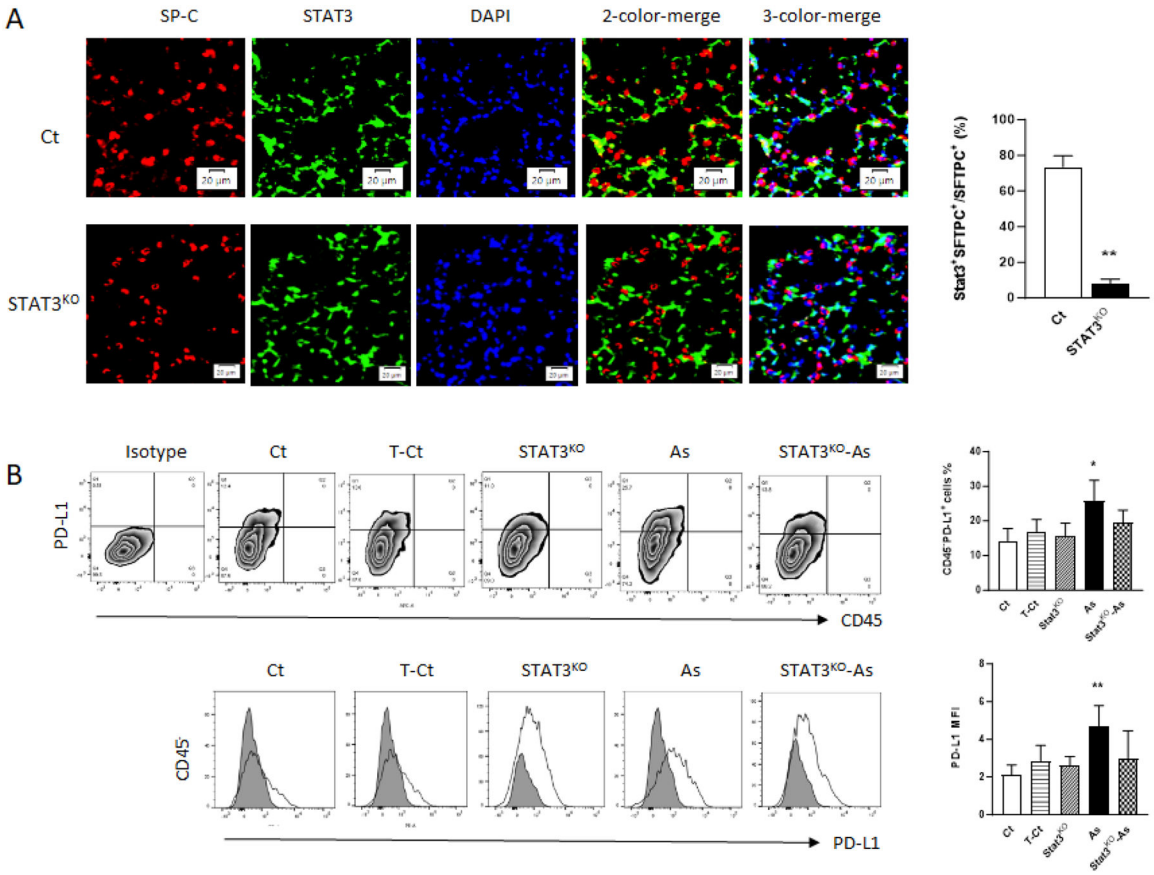

Figure 3. STAT3 mediates arsenic-induced PD-L1 upregulation in AT2 cells.

(A) Lung tissue samples from wildtype control (Ct) and STAT3 conditional KO ($STAT3^{KO}$) mice were stained with antibodies against SP-C and STAT3, respectively. The number of STAT3-possitive AT2 cells was significantly reduced in $STAT3^{KO}$ mice compared to Ct mice. N=5. **(B)** Arsenic exposure (As) induced PD-L1 up-regulation on lung tissue cells as shown by flow cytometry data compared to Ct or tamoxifen-treated control (T-Ct) mice, which was significantly reduced in arsenic-treated $STAT3^{KO}$ ($STAT3^{KO}$-As) mice. N=8. *: $p < 0.05$; **: $p < 0.01$, compared to all other groups.

Table 1.

Arsenic-enhanced lung tumorigenesis was mitigated in the mice with STAT3 KO in AT2 cells.

The mice at age of 2 months were separated into 5 groups (mice treated): wild type control (Ct), tamoxifen-treated control (T-Ct), arsenic-treated wild type (As), STAT3 conditional KO ($STAT3^{KO}$) and arsenic-treated KO ($STAT^{KO}$-As). The number of male mice in each group were shown in parenthesis. 12 months later, the mice (mice examined) were sacrificed and lung tumor status was examined. The ratio of lung/body weight, the number of mice with tumor, tumor incidence and tumor multiplicity were determined at the end of the experiment. Data for lung/body weight ratios and tumor multiplicity were presented as (mean ± SD).

Treatment Groups	Mice treated	Mice examined	Lung/bodyweight ratio, $\times 10^{-3}$	Mice with tumor	Tumor incidence	Tumor multiplicity
Ct	20 (10 ♂)	20 (10 ♂)	6.57 ± 0.54	6 (3 ♂)	30.0%	0.30 ± 0.11
T-Ct	20 (10 ♂)	20 (10 ♂)	6.S3 ± 0.88	5 (3 ♂)	25%	0.30 ± 0.13
$Stat3^{KO}$	20 (10 ♂)	19 (10 ♂)	6.60 ± 0.56	6 (4 ♂)	31.6%	0.42 ± 0.16
As	20 (10 ♂)	18 (9 ♂)	6.56 ± 0.78	14 (7 ♂)	77.8% *	1.5 ± 0.22 **
$Stat3^{KO}$-A5	20 (10 ♂)	20 (10 ♂)	6.63 ± 0.63	8 (5 ♂)	40.0%	0.50 ± 0.15

* $p < 0.05$.

** $p < 0.01$, vs all other groups.